Journal of Applied Physics

Spectrophotometric and thermal stability of agarose-based ultrasonic tissue-mimicking gel

Cite as: J. Appl. Phys. **125**, 155104 (2019); https://doi.org/10.1063/1.5082822
Submitted: 25 November 2018 . Accepted: 30 March 2019 . Published Online: 18 April 2019

Heng-Yin Chen (陳姮吟), and Nelson G. Chen (陳稷康)

Journal of Applied Physics ARTICLE scitation.org/journal/jap

Spectrophotometric and thermal stability of agarose-based ultrasonic tissue-mimicking gel

Cite as: J. Appl. Phys. **125**, 155104 (2019); doi: 10.1063/1.5082822
Submitted: 25 November 2018 · Accepted: 30 March 2019 ·
Published Online: 18 April 2019

Heng-Yin Chen (陳姮吟)[1] and Nelson G. Chen (陳稷康)[2,a)]

AFFILIATIONS

[1]Institute of Biomedical Engineering, National Chiao Tung University, Hsinchu 30010, Taiwan
[2]Department of Electrical and Computer Engineering, National Chiao Tung University, Hsinchu 30010, Taiwan

[a)]**Author to whom correspondence should be addressed:** ngchen@nctu.edu.tw

ABSTRACT

Spectrophotometric measurements of a commonly used agarose-based ultrasonic tissue-mimicking gel are reported. In addition, spectral characteristics after heating to different temperatures provide thermostability information. Thermostability of agarose gels has not been previously reported, except in general terms. Gels were produced and cast into 2 mm thick spectrophotometric cuvettes. UV-Vis spectra were recorded after gels were heated to various temperatures. Spectral changes resulting from heating were noted and were largely unchanged with heating to temperatures ranging from 30 to 70 °C. Only with heating to 80 °C, which is near the melting point of the gel material, do spectra irreversibly change. We show that agarose-based tissue-mimicking gels are largely stable over temperatures relevant to most biomedical ultrasonic studies, including those examining hyperthermia or high-intensity focused ultrasound. Therefore, they likely provide a stable substrate in which to conduct ultrasonic heating studies. In addition, UV-Vis spectrophotometry of this optically opaque material has been demonstrated. Possible additives to this material that would enable the measurement of temperature fields through postexposure sectioning and slicing are subsequently discussed.

I. INTRODUCTION

Various ultrasound phantoms have long been used to provide highly controlled and reproducible objects in research and quality assurance applications. A variety of materials have been used to produce such. Research applications include ultrasonic imaging and therapy. Phantoms contain tissue-mimicking material, which has properties similar to those of biological tissue. The most commonly used material to date for imaging studies is the agarose-based tissue-mimicking gel.[1] This solid gel, developed by Madsen *et al.*,[2] has been used for verifying the accuracy of a 3D ultrasonic imaging system[3] and ultrasound-stimulated acoustic emission frequency shifts.[4] More recently, the material was used to examine attenuation correction[5] and microbubble nonlinear propagation[6] in carotid artery flow phantoms. Nonlinear propagation in histotripsy pulses was also studied with it.[7]

The material also forms an integral part of other ultrasound phantoms that have been developed to simulate brain embedded within skull[8] and muscle surrounding bone,[9] with acrylonitrile butadiene styrene (ABS) simulating bone. Such phantoms have subsequently been used to simulate the effects of focused ultrasound on these structures.[10] Properties of this material, as previously reported,[2] are as follows: density 1.03 g/ml, ultrasonic attenuation of 0.5 dB/(cm-MHz), and sound speed 1545 m/s. Thermal conductivity of higher concentration gel is similar to that of unperfused liver.[11]

Other materials have also been developed for simulating biological tissue. They include TX-150/151 (a mixture of boric acid, guar gum, water, polyacrylamide, and triglyceride), polyacrylamide, hydroxyethyl cellulose, gelatin, gellan gum, carrageenan, and alginate. Advantages and drawbacks for each of these materials are reviewed here.[12] Polyacrylamide is the most popular material used for ultrasonic thermal studies partly due to it being clear to the eye. A key drawback though is the toxicity of its precursor acrylamide, which makes its safe fabrication more difficult. Partly due to this reason, agarose gels have also been used as an alternative in various high-intensity focused ultrasound (HIFU) studies.[13–16]

Spectrophotometry is a technique long used in chemical analysis, where both chemical identity and concentration of dissolved substances are measured. Traditionally, a dissolved sample has monochromatic light passed through it, and light levels that penetrate are recorded. Absorbance levels are proportional to chemical

species concentration and path length (Beer–Lambert law). A given species will absorb light at different wavelengths differently, characterized by its molar absorptivity, which is a function of the incident wavelength. UV-Vis spectra consist of repeated measurements of a given substance over ultraviolet and visible wavelengths of light and provide a more complete characterization of the substance than that found with a single wavelength. These spectra are usually normalized by the path length through which light traversed the sample. Given a mixture of multiple compounds, the spectra of the individual compounds add to produce the overall measured result.

Spectrophotometry of tissue-mimicking gels, as opposed to dissolved liquids, has only been attempted recently, with the development of a polyacrylamide gel that is blue when cool and reversibly becomes colorless upon heating.[17] The agarose gel investigated here is a solid mixture of agarose, milk, n-propanol, and water. Agarose is a polymer consisting of chains of alternating units of β-D-galactopyranose and 3,6-anhydro-L-galactose monomers.[18] Milk consists of mainly casein (a suspended protein) and lactose.[19] Conformational changes in polymers with temperature change usually cause changes in spectra.[20] The UV-Vis transmission spectrum of the agarose-based tissue-mimicking gel has not been previously measured, either at room temperature or upon heating. Any significant changes with the chemical properties of the material would likely be detectable as changes to spectra. If there were significant changes in the material composition, such as with a hypothetical volatile component vaporizing at elevated temperature or a permanent conformational change, the resulting spectra after cooldown would also change. A lack of change after temperature elevation and subsequent cooldown would, therefore, suggest that the material remained stable in spite of temperature elevation.

II. EXPERIMENTAL

Tissue-mimicking solid gel was produced using a formula based on that provided by Madsen *et al.*,[2] proportionally scaled to the spectrophotometric cuvette volume. In brief, agarose (Acros Organics medium-low EEO Mr = 0.12, Waltham, MA, USA), n-propanol, and distilled water were mixed in a 1 g:2 ml:23 ml ratio and heated to 90 °C until the agarose dissolved. Skimmed milk was prepared with Difco laboratory milk powder (Becton, Dickinson, and Company, Sparks, MD, USA) following the directions of the manufacturer (100 g:1 l water ratio). The mixture was subsequently allowed to cool to 55 °C at which point milk, also preheated to 55 °C, was added in a 7 (mixture):5 (milk) volumetric ratio. This combination was poured into quartz spectrophotometric cuvettes with a path length of 2 mm and allowed to cool to room temperature. The mixture solidified into its solid gel form as it cooled. Cuvettes had an internal volume of 700 μl, and external dimensions of $45 \times 12.5 \times 4.5$ mm^3. All spectrophotometric measurements were made with a range of wavelengths $\lambda = 190$–1000 nm in 1 nm increments using a spectrophotometer (Chromtech CT-2800, E-Chrom Tech Co., Ltd., Taipei, Taiwan) in order to obtain UV-Vis spectra, with samples of distilled water serving as the baseline. Gels underwent the following measurement procedure.

First, a warm water bath was preheated to 30 °C. Then, a gel was placed into it and kept for 5 min. Next, the gel was removed and allowed to cool for 5 min. Finally, the gel was placed within the spectrophotometer and had its UV-Vis spectrum (wavelengths λ ranged from 190 to 1000 nm) measured over a period of approximately 2 min 20 s. Afterward, the water bath was reset to a temperature 10 °C higher than the previous temperature and allowed to reach the newly set temperature. This measurement procedure was repeated for temperatures of 40, 50, 60, 70, and 80 °C resulting in a total of 6 spectra. The experiment was repeated five times ($n = 5$ gels) in order to assess experimental variability. Spectra were subsequently normalized by the path length of 2 mm to obtain absorptivities for analysis. Given the small gel volume, sufficient time elapsed to allow gel temperatures to reach near-equilibrium with surroundings throughout. (A side experiment and analysis are presented in the Appendix confirming this fact.) A schematic depicting the gel spectrophotometric measurement is shown in Fig. 1.

Obtained spectra after heating to each temperature were averaged and plotted. A more detailed analysis was conducted for spectra obtained after heating to temperatures of 30–70 °C at each measured wavelength. There appeared to be little difference in measured spectra at this temperature range, although there was an apparent decrease in absorptivity values at shorter wavelengths ($\lambda = 190$–350 nm) for the temperature range of 30–50 °C.

A weighted linear least squares curve fit was performed using MATLAB's Curve-Fitting Toolbox (The Mathworks, Inc., Natick, MA, USA) as follows for every wavelength. Measured absorptivities are denoted as $\{a_{30\,°C,\,1}\ a_{30\,°C,\,2}\ a_{30\,°C,\,3}\ a_{30\,°C,\,4}\ a_{30\,°C,\,5} \ldots a_{80\,°C,\,4}\ a_{80\,°C,\,5}\}$ with subscripts denoting temperature and gel number. A schematic illustrating the analysis is provided in Fig. 2.

First, any measured absorptivities of 25/cm were removed and noted, due to that value indicating light transmission values below the detection limit. Weighting was performed in order to account for possibly differing variances at each temperature. Weights w_i used were set as the reciprocal of the variance of measured data at each temperature, as suggested by the user's guide. The resulting curve fit minimizes the following sum of squares s with the y terms denoting the estimated and measured point values,

$$s = \sum_{i=1}^{n} w_i (y_i - \hat{y}_i)^2.$$

Lower and upper bounds (95% confidence intervals) of the fitted line slope were automatically computed based on the best-fit estimate

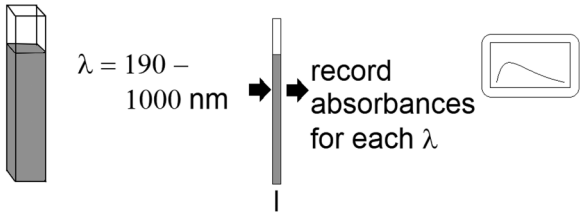

FIG. 1. Gel spectrophotometric measurement. The agarose gel is cast into a quartz spectrophotometric cuvette. Subsequently, light of various wavelengths is passed through the sample with thickness *l*, and absorbances are measured. Resulting absorbances at each wavelength (190, 191, …, 1000 nm) form a spectrum, which is subsequently normalized by path length *l* to obtain absorptivities.

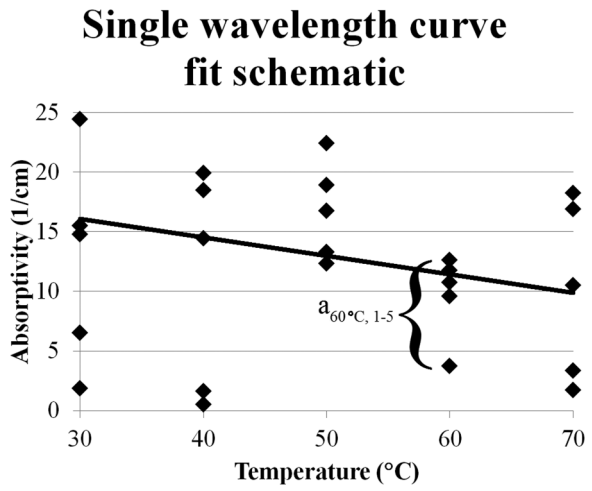

FIG. 2. Schematic of linear weighted curve fit. Data points indicating absorptivities were plotted for each temperature over specified temperature ranges (here, 30–70 °C) at one particular wavelength. Weights w_i were assigned to each set (e.g., $a_{60°C}$) of data points as the reciprocal of their variance. For any temperature, data points that are closely spaced are weighted more than points loosely spaced. The weighted least squares best-fit line was then computed, with the 95% confidence bounds of its slope noted. If there is no underlying change with temperature, the confidence bounds of the slope should span zero.

$b \pm t\sqrt{S}$, where t is the inverse of Student's cumulative distribution function and S is obtained from the estimated covariance matrix of the estimated best-fit coefficients. Wavelengths in which fitted slopes had bounds not spanning zero were noted and were considered wavelengths in which spectra changed. These bounds were plotted together with the wavelengths not spanning zero. A "region of slight change" was identified where fitted slopes were all nonzero for a continuous wavelength range. A Z-test of proportions was performed on the number of remaining wavelengths in which fitted slope confidence intervals did not span zero vs all remaining wavelengths since the appearance of these remaining wavelengths appeared to be random. This test was performed in order to determine whether these nonzero slopes occurred due to chance as opposed to being due to actual physical differences. (On average, given no underlying difference, there will be 1/20 95% confidence intervals that fail to span zero.)

A subsequent analysis in which data from only 30–50 °C were used was performed in order to ascertain whether there were statistically significant changes over this reduced temperature range. The analysis was performed using the same procedure described above with weighted linear least squares curve fits for the shorter wavelengths ($\lambda = 190$–350 nm) in question, with fitted slopes and their lower and upper bounds at 95% confidence recorded.

Differences between the 70 °C and 80 °C spectra were computed and two sample heteroscedastic t-tests performed for each wavelength in order to determine regions where differences were significant ($p < 0.05$). Average differences were plotted and wavelengths with significant differences noted.

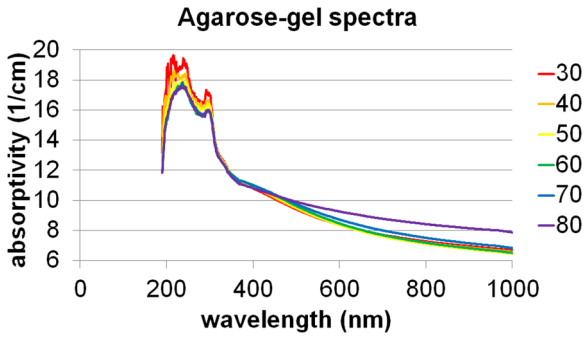

FIG. 3. Change in tissue-mimicking gel absorption UV-Vis spectra upon heating from 30 to 80 °C. Colored lines denote average spectrophotometric absorptivities at each temperature in °C ($n = 5$, exceptions noted in the text). It is apparent that an increase in absorption occurs at longer wavelengths upon reaching 80 °C while little change occurs at lower temperatures.

III. RESULTS

Average UV-Vis absorptivity spectra of the agarose-based tissue-mimicking gel material were computed based on a series of five measurements at each temperature with exceptions noted below and shown in Fig. 3.

A few individual measurements exceeded the maximum detectable absorbance of 5, corresponding to an absorptivity of 25 (1/cm) for the 30 °C case; therefore, these measurements were excluded from the plot. The wavelengths where such occurred and the number of remaining valid points used to compute the mean are as follows ($\lambda = 190$, 193–200, 205–206, 221 nm, $n = 4$; $\lambda = 207$–210 nm, $n = 3$). There appears to be little change in the UV-Vis spectrum with heating up to 70 °C. However, there is a marked increase in absorptivity at longer wavelengths when 80 °C is reached. At no point going from 30 to 80 °C did the gel appear differently in terms of gross visual appearance. Specific heat capacity was estimated to be 4.1 J/(g °C) using a weighted average of that of water and milk, where the two components compose around 95% of the overall phantom.[10]

A. Stability from 30 to 70 °C

Fitted lower and upper bounds for fitted line slopes at all wavelengths are summarized in Fig. 4. If the region of slight change with statistically significant differences (399–509 nm) is excluded, there are 700 remaining wavelengths. With these 700 wavelengths, one expects repeated examination of 95% confidence bounds to produce an expected $700/20 = 35$ wavelengths with confidence bounds that do not span zero even when no underlying difference exists. Actual data contained 30 such wavelengths. One-proportion Z-testing indicates that this result (30 observed tests with 35 expected tests, $n = 700$) is consistent ($p = 0.3539$) with no underlying difference.

Representative sample plots of measured absorptivities as a function of temperature are shown in Fig. 5. The weighted least squares fitted line slopes do not substantially differ from zero, indicating that the gels were largely stable over this temperature range. Estimated slopes and their confidence bounds for the sample plotted wavelengths are given in Table I.

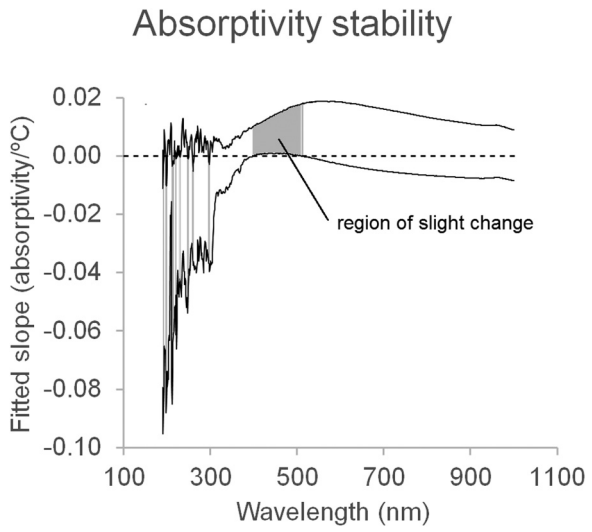

FIG. 4. Slope 95% confidence bounds for all measured wavelengths. Shaded areas indicate wavelengths where the fitted slope's bounds did not include zero. The only region where such repeatedly occurs ranges from 399 to 509 nm, which has been labeled the region of slight change. Other wavelengths where the slope 95% confidence bounds do not span zero only sporadically appear. The dashed line indicates zero slope.

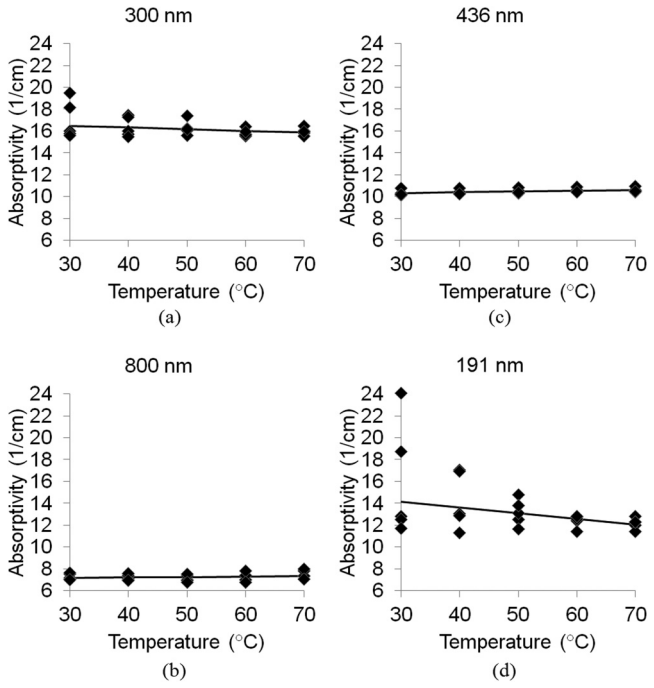

FIG. 5. Absorptivity at various wavelengths from 30 to 70 °C. Little change occurs over this temperature range. (a) and (b) At 300 and 800 nm, where typical behavior is observed, the fitted straight line slope is indistinguishable from zero, indicative of no change. Elsewhere, where the slope differs from zero at the 95% confidence level, the difference is nonetheless slight for a usual case (436 nm) in the region of slight change (c). (d) The largest deviation from 0 slope was found to occur at 191 nm, and even here the deviation was not large.

Examination of the results at 436 nm, which is in the region of slight change where statistically significant (as determined by the estimated slope's 95% confidence interval not spanning zero) differences were present, nonetheless indicates that said differences are unlikely to have practical implications. The expected change due to the largest temperature change (70 – 30 °C = 40 °C) on absorptivity is merely 0.28. At that wavelength, the absorptivity is ca. 10 (1/cm), which translates to a 2.8% difference. Other parameters would produce similar or lesser differences. Summary statistics for the region are as follows (absorptivity/°C): mean value 0.0075; mean lower and upper bound values are 0.0006 and 0.0143, respectively. In other words, there was a statistically significant difference that is in practice negligible.

Although there is an apparent decrease in the short wavelength region (λ = 190–350 nm) with heating from 30 °C to 50 °C, analysis of line fits of absorptivities recorded for these temperatures reveals that the decreases were not statistically significant. All fitted slopes had 95% confidence intervals that spanned zero. Summary statistics are as follows: n = 161 wavelengths, mean slope −0.0318, mean lower bound −0.1009, and mean upper bound +0.0373 (all in absorptivity/°C). The lack of statistical significance at these wavelengths is due to the relatively high noise present at these wavelengths vs those of longer wavelengths, leading to the apparent decrease in absorptivities. One observes this larger noise, and hence dispersion, in Fig. 5(d).

B. Change from 70 to 80 °C

The average absorption difference going from 70 to 80 °C and computed standard deviations indicate that the difference becomes significant ($p < 0.05$) for all wavelengths longer than 600 nm and that the difference grows with increasing wavelength. This result is illustrated in Fig. 6. In practical ultrasonic applications, such high temperatures are less likely to be reached, indicating the stability of the agarose-based tissue-mimicking gel.

IV. DISCUSSION

Agarose-based tissue-mimicking gels have previously been described as thermally stable based on its high melting point, yet their stability had not been more rigorously characterized. In conventional ultrasonic hyperthermia studies where tissue is heated to elevated temperatures to treat disease, the temperatures reached are around 40–46 °C.[21] In high-intensity focused ultrasound (HIFU), spot sizes reach temperatures of approximately 60 °C, triggering coagulation necrosis, although higher temperatures are possible.[22] Our demonstration of the stability of the agarose-based tissue-mimicking gel over a temperature range expected to cover both hyperthermia and HIFU means that exposing the gel to these modalities is not expected to produce effects arising from the gel itself. Agarose gel likely provides a temperature stable tissue-mimicking substrate for most experimental studies. Our measurements up to 80 °C span the temperature ranges likely to be reached

TABLE I. Sample fitted slopes and 95% confidence bounds.

Wavelength (nm)	Value (absorptivity/°C)	Lower bound	Upper bound	Notes
300	−0.015 8	−0.036 9	0.005 2	
800	0.003 333	−0.006 6	0.013 3	
436	0.006 979	0.000 852 3	0.013 11	In region of slight change
191	−0.053 21	−0.095 34	−0.011 08	Largest deviation from 0

in ultrasonic studies. One rare example of HIFU leading to temperatures beyond the stable temperature limit around 70 °C is the liver hemostasis study[23] in which maximum temperatures reached 86 °C.

However, one limitation of the present study is its inability to exclude the possibility of *reversible* conformational changes that revert upon cooling to room temperature that take place with gel heating. Heating to various temperatures can cause individual polymer chains of the agarose and/or casein to undergo conformational change themselves, and/or alter their relationships with other polymer chains that are present. These changes would then revert upon cooling to room temperature, rendering them undetectable with the described experimental apparatus. The permanent spectral changes observed with heating to 80 °C indicate that irreversible changes occur near the melting point, but not prior to that. Hypothetical reversible conformational changes can change gel behavior and material properties at temperatures between 30 and 70 °C and further work is required to either demonstrate or exclude their existence. Explanations of individual absorptivities in observed spectra after heating to 30–70 °C and their change after heating to 80 °C also require additional study to elucidate.

It is possible to perform experimental studies into ultrasonic heating within tissue using the agarose gel. Efforts have been made to measure temperature rises within tissue phantoms. A polyacrylamide gel phantom with embedded irreversible thermochromic ink has been developed that changes color around 60 °C and upon close examination indicates temperature gradients.[24] Bovine serum albumin (BSA) can be added to polyacrylamide gels in which temperature change causes a transformation from transparent to opaque between 50 and 60 °C. The temperature at which the change occurs can be adjusted through control of pH.[25] This approach was used to measure the effect of ultrasound contrast agents on thermal lesions.[26] Polyacrylamide phantoms are visually clear, which allows one to visually detect regions with maximal heating, especially with temperature sensitive additives like thermochromic ink and BSA. The agarose gel is opaque to the naked eye; however, our demonstration of the successful measurement of its spectra for 2 mm thin samples suggests that it is also possible to measure temperature rises in three dimensions through the addition of similar additives as that used for polyacrylamide gels in an approach similar to that developed by Appleby and Leghrouz[27] for ionizing radiation. In short, their work showed that agarose gels containing radiation-sensitive additives change color upon exposure. Fields postexposure are subsequently identified through spectrophotometry of gel slices. For ultrasonic heating, changes to temperature sensitive additives would be likewise measured with spectrophotometry. Separate work including additives to the gel is described in other papers being prepared.

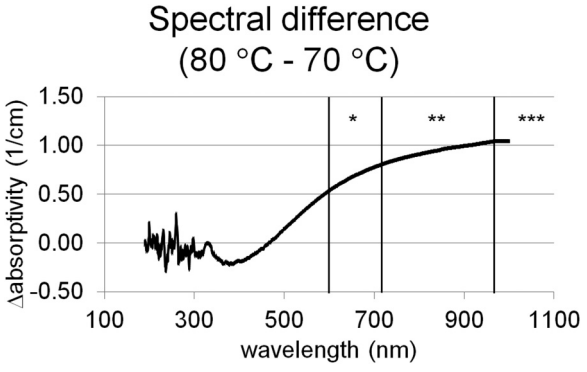

FIG. 6. Spectral differences occurring due to heating to 80 °C vs 70 °C. The differences in measured spectra are statistically insignificant ($p > 0.05$), as determined through t-tests at each wavelength, for wavelengths less than 600 nm, and are significant otherwise. Asterisks denote p-value ranges (*p between 0.05 and 0.01, **p between 0.01 and 0.001, ***p less than 0.001).

V. CONCLUSIONS

Spectrophotometry of the agarose-based tissue-mimicking gel has been successfully performed for 2 mm thin slices at varying temperatures. The material spectra do not appreciably change after heating to 30–70 °C, which is likely indicative of the material stability at elevated temperatures. This temperature range spans temperatures expected with ultrasonic thermal studies. Therefore, the agarose-based tissue-mimicking gel provides a stable substrate for various ultrasonic heating studies. The ability to measure gel spectra suggests a means for quantifying ultrasonically induced temperature fields.

ACKNOWLEDGMENTS

This work was supported in part from a grant from the Ministry of Science and Technology (MOST) (No. MOST 105-2221-E-009-094) of the Republic of China (Taiwan).

APPENDIX: SUFFICIENCY OF HEATING AND COOLING TIME FOR GEL TO APPROACH STATED TEMPERATURES

Analysis of gel temperature changes over the time periods in which the gel was allowed to warm and cool are as follows. In summary, it is shown that the 5 min intervals during which the gel warmed and cooled was sufficient to cause the material to approach target temperatures (e.g., placing the gel into an 80 °C water bath for 5 min causes the gel temperature to become approximately equal to 80 °C). Heating and cooling rates were experimentally determined

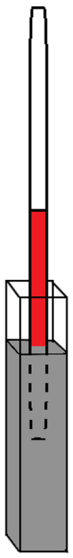

FIG. 7. Agarose gel cast into a cuvette with an embedded laboratory thermometer. The thermometer allowed continuous monitoring of the gel temperature over time. The cuvette used for these side measurements was one with standard dimensions (1 cm interior length and width, 45 mm height) in order to accommodate the embedded thermometer.

for a quartz cuvette holding the agarose gel, with an embedded thermometer as shown in Fig. 7.

Placing the thermometer-containing gel into a water bath preheated to 80 °C and monitoring the resulting temperature rise over time indicate that the gel reached a measured temperature of 80 °C in 130 s ($n = 2$). For the thin 2 mm path thickness cuvette used in the experiment presented in the main work, the heating rate for the gel could only be faster because of the following:

1. There was only 1/5th the gel material to be heated (1 cm path length for this study vs 2 mm path length for the main work).
2. However, the surface area ratio was 0.6 (equal gel height, a perimeter of 4 cm in this study vs 2.4 cm in the main work), so the heating would be faster overall when accounting for both the decreased surface area and increased quantity of gel.
3. Measurement of heating to 80 °C is indicative of the "worst-case," i.e., if the heating rate is sufficient to reach 80 °C over 5 min, it is sufficient to reach any temperature less than 80 °C over the same time period.

Heat transfer is modeled through a convective mechanism, with the heat transfer rate proportional to surface area.

Measurement of gel cooling from the heated state back to room temperature was performed by heating the 1 cm^2 gels to 70 °C with a water bath, and subsequently removing them to still air at room temperature with monitoring of their temperature decrease over 5 min. Temperature decreases are plotted in Fig. 8.

These measured curves were fit to a decaying exponential function using MATLAB in the form $A^*\exp(-Bt) + 25$, with fitted

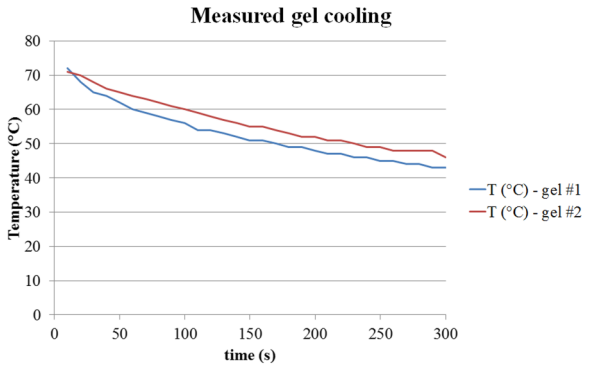

FIG. 8. Cooling measurements of agarose gel in a standard quartz cuvette, obtained through an embedded thermometer.

parameters A and B noted. (The constant 25 accounts for a room temperature of 25 °C.)

Newton's law of Cooling[28] states that the instantaneous heat flux $q''(t)$ is equal to $h(T_S(t) - T_\infty)$, where h is the convection heat transfer coefficient, $T_S(t)$ refers to the object temperature, and T_∞ is the temperature of the object surroundings. From the specific heat capacity of the gel of 4.1 J/(g °C) and its volume ($3 \times 1 \times 1$ $cm^3 = 3$ ml) and density of 1 g/ml, a total of 554 J of energy needs to be transferred out of the 70 °C gel to the surrounding air in order for its temperature to fall to 25 °C. On a per unit surface area (3 cm height × 1 cm × 4 sides = 12 $cm^2 = 0.0012$ m^2) basis, the required energy is 461 667 J/m^2. Integrating the instantaneous heat flux equation with respect to time provides the following:

$$q''(t) = h(T_S(t) - T_\infty) = h(T_{diff}(t)) = hAe^{-Bt}$$

$$\int_0^\infty q''(t)dt = h\int_0^\infty T_{diff}(t)dt = \frac{hA}{B} = 461\,667\ \mathrm{J/m^2}.$$

The integral gives the total energy transferred per unit surface area. Substituting fitted values of A and B obtained from measured data above provides estimates of the convection heat transfer coefficient h for our case of a quartz cuvette placed in air. The results are provided in Table II.

For the gel described in the main work which had a thickness of 2 mm rather than 1 cm, there is 1/5 of the gel material to cool with 0.6 times the surface area as described above. So, the total energy transfer required to cool from 70 °C to room temperature of 25 °C is 111 J. On a per unit area basis, it is 154 166 J/m^2. Define T_{excess} as the temperature of the gel in excess of room temperature

TABLE II. Heat transfer coefficient estimates.

Parameter	Gel #1	Gel #2	
A (°C)	44.201	46.05	
B (1/s)	0.003 271 6	0.002 664 1	
h (W/(m^2 °C))	34	27	Average = 31

TABLE III. Estimated T_{excess} after 5 min room temperature air exposure.

Temperature (°C) at $t = 0$	30	40	50	60	70	80
T_{excess} (°C) at 5 min	0.3	1.0	1.6	2.3	3.0	3.6[a]

[a]Due to changes in the chemical composition of the gel upon heating to 80 °C as evidenced by the change in its spectrophotometric spectrum as detailed in the main text, this particular estimate of T_{excess} is less precise than the other estimated values. Nevertheless, T_{excess} always was within a few degrees of room temperature.

($T_{excess} = T_{gel} - T_{room}$). Again integrating the instantaneous flux equation with respect to time provides

$$\int_0^\infty q''(t)dt = h\int_0^\infty T_{excess}(t)dt = 154\,166\,\mathrm{J/m^2}.$$

With the earlier average estimate of $h = 31$ W/(m^2 °C) and $T_{excess}(t) = 45\exp(-Bt)$, B is estimated to be 0.0090 (1/s). At 5 min, T_{excess} is estimated then to be 3.0 °C. Following the same procedure for the other temperatures examined provides the estimates given in Table III.

REFERENCES

[1]M. O. Culjat, D. Goldenberg, P. Tewari, and R. S. Singh, Ultrasound Med. Biol. **36**, 861 (2010).
[2]E. Madsen, G. R. Frank, and F. Dong, Ultrasound Med. Biol. **24**, 535 (1998).
[3]G. M. Treece, A. H. Gee, R. W. Prager, C. J. C. Cash, and L. H. Berman, Ultrasound Med. Biol. **29**, 529 (2003).
[4]E. Konofagou, J. Thierman, and K. Hynynen, Ultrasonics **41**, 337 (2003).
[5]W. K. Cheung, D. M. Gujral, B. N. Shah, N. S. Chahal, S. Bhattacharyya, D. O. Cosgrove, R. J. Eckersley, K. J. Harrington, R. Senior, C. M. Nutting, and M. X. Tang, Ultrasound Med. Biol. **41**, 1876 (2015).
[6]Y. O. Yildiz, R. J. Eckersley, R. Senior, A. K. P. Lim, D. Cosgrove, and M. X. Tang, Ultrasound Med. Biol. **41**, 1938 (2015).
[7]K. B. Bader, M. J. Crowe, J. L. Raymond, and C. K. Holland, Ultrasound Med. Biol. **42**, 1701 (2016).
[8]G. Menikou, T. Dadakova, M. Pavlina, M. Bock, and C. Damianou, Ultrasonics **57**, 144 (2015).
[9]G. Menikou, M. Yiannakou, C. Yiallouras, C. Ioannides, and C. Damianou, Ultrasonics **71**, 12 (2016).
[10]G. Menikou and C. Damianou, J. Ther. Ultrasound **5**, 14 (2017).
[11]E. Mylonopoulou, M. Bazán-Peregrino, C. D. Arvanitis, and C. C. Coussios, Int. J. Hyperthermia **29**, 133 (2013).
[12]A. Dabbagh, B. J. J. Abdullah, C. Ramasindarum, and N. H. A. Kasim, Ultrason. Imaging **36**, 291 (2014).
[13]R. G. Holt and R. A. Roy, Ultrasound Med. Biol. **27**, 1399 (2001).
[14]J. Huang, R. G. Holt, R. O. Cleveland, and R. A. Roy, J. Acoust. Soc. Am. **116**, 2451 (2004).
[15]C. H. Farny, R. G. Holt, and R. A. Roy, IEEE Trans. Biomed. Eng. **57**, 175 (2010).
[16]R. Ortega, A. Téllez, L. Leija, and A. Vera, Phys. Procedia **3**, 627 (2010).
[17]A. Dabbagh, B. J. Abdullah, N. H. Abu Kasim, and C. Ramasindarum, Int. J. Hyperthermia **30**, 66 (2014).
[18]R. Armisen and F. Galatas, FAO Fisheries Technical Paper No. 288, 1987.
[19]*Bergey's Manual of Systematic Bacteriology*, edited by P. H. A. Sneath and J. G. Holt (Williams & Wilkins, 1986), p. 2.
[20]K. Gosa, D. Donescu, and N. Carp, Makromol. Chem. **182**, 1725 (1981).
[21]K. Hynynen, D. Shimm, D. Anhalt, B. Stea, H. Sykes, J. R. Cassady, and R. B. Roemer, Int. J. Hyperthermia **6**, 891 (1990).
[22]T. J. Dubinsky, C. Cuevas, M. K. Dighe, O. Kolokythas, and J. H. Hwang, Am. J. Roentgenol. **190**, 191 (2008).
[23]S. Vaezy, R. Martin, U. Schmiedl, M. Caps, S. Taylor, K. Beach, S. Carter, P. Kaczkowski, G. Keilman, S. Helton, W. Chandler, P. Mourad, M. Rice, R. Roy, and L. Crum, Ultrasound Med. Biol. **23**(9), 1413 (1997).
[24]A. H. Negussie, A. Partanen, A. S. Mikhail, S. Xu, N. Abi-Jaoudeh, S. Maruvada, and B. J. Wood, Int. J. Hyperthermia **32**, 239 (2016).
[25]M. McDonald, S. Lochhead, R. Chopra, and M. J. Bronskill, Phys. Med. Biol. **49**, 2767 (2004).
[26]C. Lafon, A. Murillo-Rincon, C. Goldenstedt, J. Y. Chapelon, F. Mithieux, N. R. Owen, and D. Cathignol, Ultrasonics **49**, 172 (2009).
[27]A. Appleby and A. Leghrouz, Med. Phys. **18**, 309 (1991).
[28]F. P. Incropera and D. P. DeWitt, *Fundamentals of Heat and Mass Transfer*, 4th Ed. (Wiley, 1996), p. 8.